Synthesis of nano-sized hydrocalumite from a Gastropod shell for aqua system phosphate removal

ARTICLE *in* SEPARATION AND PURIFICATION TECHNOLOGY · MARCH 2014

Impact Factor: 3.09 · DOI: 10.1016/j.seppur.2014.01.018

5 AUTHORS, INCLUDING:

N. A. Oladoja
Adekunle Ajasin University
44 PUBLICATIONS **405** CITATIONS
SEE PROFILE

Adelagun Ruth
Federal University Wukari
8 PUBLICATIONS **21** CITATIONS
SEE PROFILE

Isaac Ololade
Adekunle Ajasin University
35 PUBLICATIONS **148** CITATIONS
SEE PROFILE

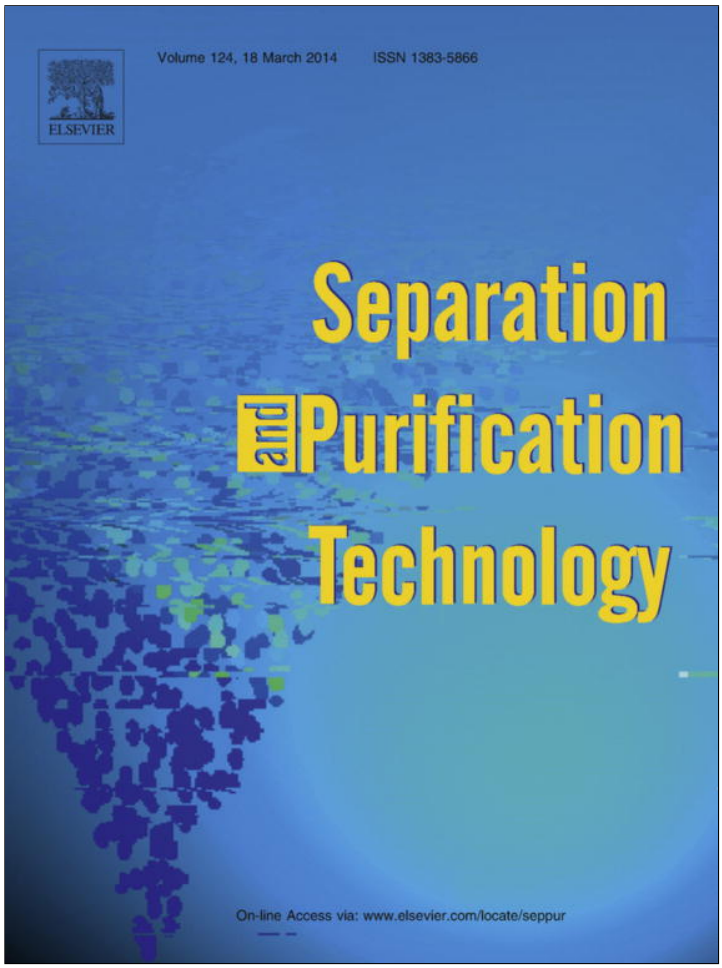

Separation and Purification Technology 124 (2014) 186–194

Contents lists available at ScienceDirect

Separation and Purification Technology

journal homepage: www.elsevier.com/locate/seppur

Synthesis of nano-sized hydrocalumite from a Gastropod shell for aqua system phosphate removal

N.A. Oladoja [a,*], R.O.A. Adelagun [b], I.A. Ololade [a], E.T. Anthony [a], M.O. Alfred [a]

[a] Department of Chemistry, Adekunle Ajasin University, Akungba Akoko, Nigeria
[b] Department of Chemical Sciences, Federal University, Wukari, Nigeria

ARTICLE INFO

Article history:
Received 14 November 2013
Received in revised form 13 January 2014
Accepted 21 January 2014
Available online 28 January 2014

Keywords:
Hydrocalumite
Phosphate removal
Eutrophication control
Supersaturation index
Calcium phosphate

ABSTRACT

Material with high affinity for oxyanions, Hydrocalumite (HC), was synthesized using a waste biogenic resource as a precursor and its ability to remove phosphate from aqua system was studied. The synthesis of HC samples with particle sizes that ranged between 116 and 135 nm was confirmed by XRD analysis. High correlation coefficient values (r^2 = 1.000) were obtained when the time–concentration profile data were fitted to the pseudo second order kinetic model. The formation of supersaturated Ca and Al phosphate salts were confirmed by the positive saturation index values and the feasibility of precipitate formation by the supersaturated salts were confirmed by the thermodynamic parameters (i.e. $\Delta G < 0$). Process variables optimization (pH, ionic strength and organic load) had nominal influence on the magnitude of phosphate removal. The fractionation of the phosphate laden HC (PHC_2) showed that the greater percentage (>99%) of the phosphate was distributed within the calcium matrix. Comparison of the EDAX spectra of the virgin HC with the PHC_2 showed that anion exchange could also be a player in phosphate removal by the HC.

1. Introduction

Hydrocalumite (HC) is a member of an emerging material of choice in diverse uses, referred to as layered double hydroxides (LDH). The LDH compounds are the only known family of the layered solids with positively charged layers, and this electrical property play an important role on the performance of the compounds [1]. LDHs are well documented as effective ion exchangers/adsorbents for removal of a variety of anionic pollutants [2]. The choice of HC as a potential reactive material for phosphate removal from aqueous media was predicated on the low-cost of methods of preparation and the plethora of reports on its excellent ability to immobilize oxyanions from aqua system [3–11]. Chrysochoou and Dermatas [6] have also established that HC is more suitable than Ettringite for oxyanion immobilization. The high affinity of HC for oxyanions have been ascribed to the Friedel phase (i.e. $Ca_2Al(OH)_6Cl(H_2O)_2{\cdot}mH_2O$, -chloride hydrocalumite), which is susceptible to Cl^- corrosion. It was assumed that since Cl^- has less affinity for HC than majority of oxyanions, it is believed that the ion substitution of Cl^- with other oxyanions ensue easily.

A Gastropod shell, African Land Snail (*Achatina achatina*) shell (SS), is being proposed as a source of M^{2+} (Ca^{2+}) for HC synthesis because of the inherent chemical and mineralogical assemblage [12,13]. In addition, Gastropods have worldwide distribution from the near arctic and Antarctic zones to the tropics and they are very striking in its extraordinary diversification of habitats. Large tonnes of Gastropod shell are discharged annually, as waste from food processing industries, which made it a low cost and abundant material that could be harnessed for deriving Ca^{2+} [14]. The use of SS as a Ca^+ ion source in environmental remediation and material synthesis have been reported [14,15]. Mollusks make up the phylum Mollusca and Gastropoda (snails and slugs) is a class under the phylum Mollusca. The snail shell has got the same basic construction as other Mollusk shells and it contains, mainly, $CaCO_3$, as well as various organic compounds [12,13].

In the present studies, we report, for the first time, the synthesis and characterization of HC from a Gastropod shell. This waste biogenic precursor was selected from the perspective of value addition to waste and cost minimization in material synthesis, for low-cost remediation of phosphate contaminated aqueous system, especially in the developing regions of the world. The ability of the synthesized HC in the removal of phosphate from aqueous solution was systematically studied. The kinetic and isotherm parameters were calculated and the mechanism of interaction between the HC and phosphate was elucidated. The distribution of phosphate moieties in the HC was studied to gain insight into the possible mechanism of phosphate removal and the role of different constituents of the HC in the phosphate removal process.

* Corresponding author. Tel.: +234 8055438642.
E-mail address: bioladoja@yahoo.com (N.A. Oladoja).

http://dx.doi.org/10.1016/j.seppur.2014.01.018
1383-5866/

2. Materials and methods

2.1. HC synthesis and characterization

Solution of $CaCl_2$ was derived from the SS, as described in our previous study [16]. The hydrocalumite was prepared by the co-precipitation method, using $AlCl_3$ as the source of Al thus: mixed solutions containing the appropriate mass ratios of Ca:Al (1, 2 and 4) were prepared and stirred to obtain an even mix. The mixture was agitated thoroughly before another solution containing 2 M NaOH was added under vigorous stirring. The slurry was allowed to gelate in the mother liquor for 24 h, at ambient temperature, before it was washed severally with deionized water. The slurry was collected and allowed to dry to constant weight in the drying oven at 80 °C. The synthesized HC were labeled HC_1; HC_2 and HC_4, the subscript showing the Ca:Al ratio used in the synthesis.

The crystallinity and mineralogical assemblage of the HC samples were determined via X-ray diffraction (Philip PW 1820 diffractometer). Diffraction patterns of the samples were recorded with Cu Kα radiation (λ = 1.54060 Å) and recorded in the range of 5–90° (2 theta) with a scanning rate of 2°/min and a step size of 0.01.

The surface morphology and elemental composition were determined by scanning electron microscopy (SEM) equipped with energy dispersive X-ray (EDX). The analysis was carried out using a scanning electron microscope (Model EMJEOL-JSM6301-F) with an Oxford INCA/ENERGY-350 microanalysis system. The EDX microanalysis system (Oxford INCA 400, Germany) was connected to the SEM machine. The EDX analysis used Mn Kα as the energy source operated at 15 kV of accelerating voltage, 155 eV resolutions and 22.4° take off angle.

Fourier transformed infrared spectroscopy (FTIR) analyses were performed on the samples to determine the functional groups present. The samples and analytical grade KBr were dried at 100 °C overnight prior to the FTIR analysis. A mixture of 0.25 mg of each sample and 100 mg of KBr was ground to fine particles and was placed in a manually operated hydraulic press operated at 8 Mbar to obtain a translucent disc of 12.7 mm diameter and about 1 mm thickness. The instrument used was Perkin–Elmer Spectrum GX Infrared Spectrometer with resolution of 4 cm^{-1} operating in the range of 4000–400 cm^{-1}. The pH_{PZC} was determined via a batch equilibrium procedure described by Milonjić et al. [17].

2.2. Phosphate uptake studies

The kinetic parameters of phosphate sorption onto the HC were derived by the addition of 2.0 g of HC into a liter of phosphate, derived from potassium dihydrogen phosphate (KH_2PO_4), solution of concentrations that ranged between 25 and 300 mg/L. Samples were withdrawn at intervals between 0 and 3 h, of sorption, centrifuged and the supernatant phosphate concentration was determined in each case. The equilibrium isotherm analysis of the sorption of phosphate by the HC samples was evaluated by contacting 50 ml solution of known phosphate concentration that ranged between 25 and 300 mg/L with 0.1 g of HC. The mixture was stirred at 200 rpm in thermostatic shaker for 2 h, samples were removed, centrifuged and the supernatant was analyzed for residual phosphate (expressed as phosphorous) by the molybdenum-blue ascorbic acid method with a UV–VIS spectrophotometer (at λ_{max} = 880 nm). The amount of phosphate sorbed per unit mass of the HC (in mg/g) was calculated using the mass balance procedure [18].

The influence of some process variables on the sorption process were evaluated thus: the effects of pH on the sorption process was investigated by varying the pH of the initial phosphate solution between pH 7 and 10; the effects organic interference was simulated by the addition of humic acid (HA) of concentrations that range between 5 and 80 mg/L. The ionic strength effect was tested using NaCl solutions of the different concentrations, equivalent to the following ionic strengths (mol/L): 0.0215; 0.04275; 0.0855; 0.171 and 0.4275.

2.3. Fractionation of phosphate laden HC

The forms and pattern of phosphate distribution in the HC reactor was studied via a protocol initially proposed by Chang and Jackson [19] and subsequently modified by Gu and Jiang [20]. Phosphate saturated HC was obtained by weighing 10.0 g of HC into a 1 L Erlenmeyer flask, and 500 ml of phosphate solution (500 mg/L) was then added, and agitated for 24 h. The phosphate adsorbed HC was washed with distilled water until no phosphate can be detected in the filtrate and dried at 40 °C for 8 h. Total P (TP) was analyzed by calcinations of 0.5 g of phosphate laden HC at 450 °C for 3 h, and subsequent extraction was carried out for 16 h with 3.5 M HCl. The TP in the extracts was measured by the molybdenum blue method with a spectrophotometer. P-saturated HC (0.5 g in dry weight) was added into 50-ml polyethylene centrifuge tubes containing 25 ml of 0.25 M $NaHCO_3$ (pH 7.5). The mixture was shaken on an orbital shaker at 25 °C for 1 h, and the supernatant was separated by centrifugation. The supernatant was filtered before the dicalcium phosphate (Ca_2-P) concentration was determined. The residue was washed twice with 95% ethanol (each wash was 12.5 ml). The supernatant was centrifuged and discarded before 25 ml of 0.5 M NH_4Ac (pH 4.2) was added. The mixture was left to stand for 4 h, which allowed the residue to thoroughly scatter during this time. The mixture was shaken for 1 h at 25 °C and then by centrifuged. The supernatant was then filtered before the octacalcium phosphate (Ca_8-P) concentration was determined. The residue was washed twice with saturated NaCl (each wash was 12.5 ml). The supernatant was centrifuged and discarded before 25 ml of 0.5 M NH_4F (pH 8.2) was added. The mixture was then shaken for 1 h at 25 °C followed by centrifugation, and the supernatant was filtered before the determination of aluminum phosphate (Al-P). The residue was subsequently extracted by 25 ml of 0.5 M H_2SO_4, and the mixture was shaken for 1 h at 25 °C followed by centrifugation and filtration of the supernatant before analysis of ten-calcium phosphate (Ca_{10}-P).

3. Results and discussion

3.1. Sorbent characterization

The XRD pattern (Fig. 1) of HC_2 and HC_4 samples agreed with that recorded in the database of the International Center for Diffraction Data, which confirmed that these materials are hydrocalumites. Series of sharp and intense symmetric peaks at low 2θ values and small symmetric peaks at high 2θ values revealed characteristic basal reflections, which has been ascribed to the LDH-type materials [21]. The values of the d-spacing, obtained for samples HC_2 and HC_4, were typical of that of the synthesized HC reported by other workers, [2,11,21]. The positions and the relative intensity of the peaks shown by samples HC_2 and HC_4 were very similar while sample HC_1 differed in both the relative intensity and peak positions and value of lattice spacing. Samples HC_2 and HC_4 showed the characteristic 2θ reflection at 11.07 and 11.22 with the d-spacing value at 7.99 Å and 7.88 Å, respectively, while sample HC_1 did not show any of these peaks and lattice spacing values. The other major reflections of HC shown by HC_2 and HC_4 are 3.95 Å and 3.93 Å at 2θ values of 22.52, and 22.60 and 2.84 Å and 2.88 Å at 2θ values of 31.52 and 31.04 respectively.

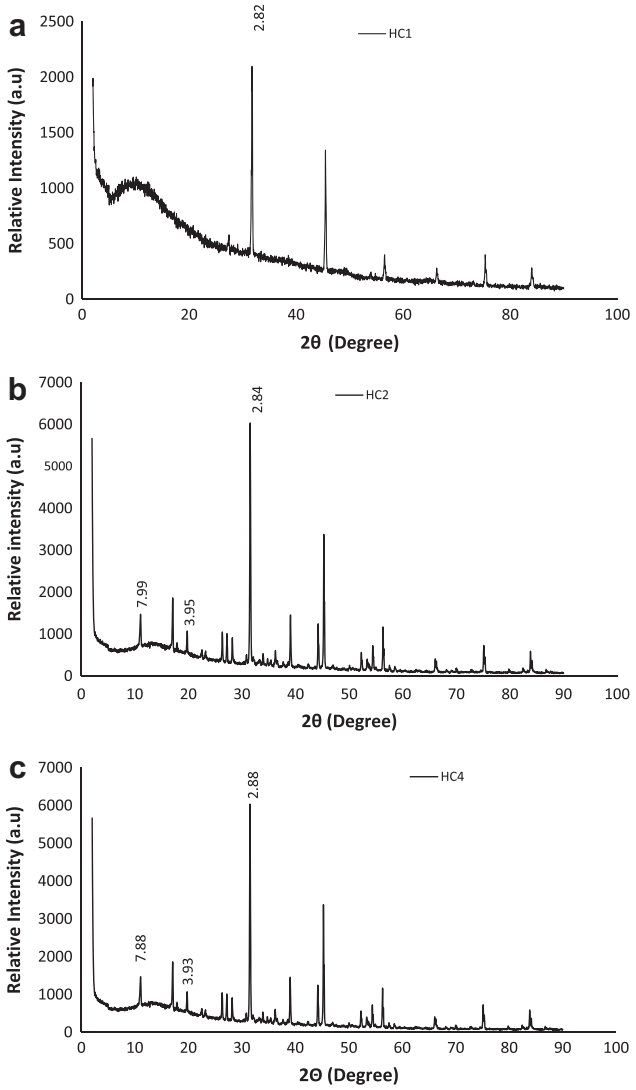

Fig. 1. (a) Powdered XRD pattern of the synthesized HC_1 sample, (b) powdered XRD pattern of the synthesized HC_2 sample, and (c) powdered XRD pattern of the synthesized HC_4 sample.

Some other peaks that are uncharacteristic of the LDH were also observed and these were attributed to the presence of impurities in the samples, originating from the biogenic precursor. The size of the particles of the synthesized HC samples were calculated using Scherrer equation; $D = 0.9\lambda/\beta \cos\theta$, where λ is the wavelength of X-rays, β, is the half width at full maximum and, θ, is the diffraction angle. The average grain size of the particles (nm) was found to be 135.26, 116.12, and 121.60 for HC_1, HC_2 and HC_4, respectively.

The results of the SEM and EDX analysis of the HC samples are presented in Fig. 2a–f. The SEM analysis showed that the samples are made up of particles of irregular shapes and sizes. The pore locations and sizes are also asymmetrical. Sample HC_1 appeared as a fusion of relatively larger particles, whereas the other two samples (sample HC_2 and HC_4) appeared as being derived from smaller particle sizes. The results of the EDX analysis revealed the prominence of Ca, Al, Cl, and O in all the samples. The ratio of calcium to aluminum recorded (HC_1:3.19; HC_2:4.37; HC_4:6.79), via the EDX analysis increased with increase in the initial Ca/Al concentration ratio used in the synthesis. The HC samples are the presence of Na observed in all the samples was attributed to the residual Na from the NaOH solution, used as precipitant, while the trace of Si observed was attributed to the biogenic precursor.

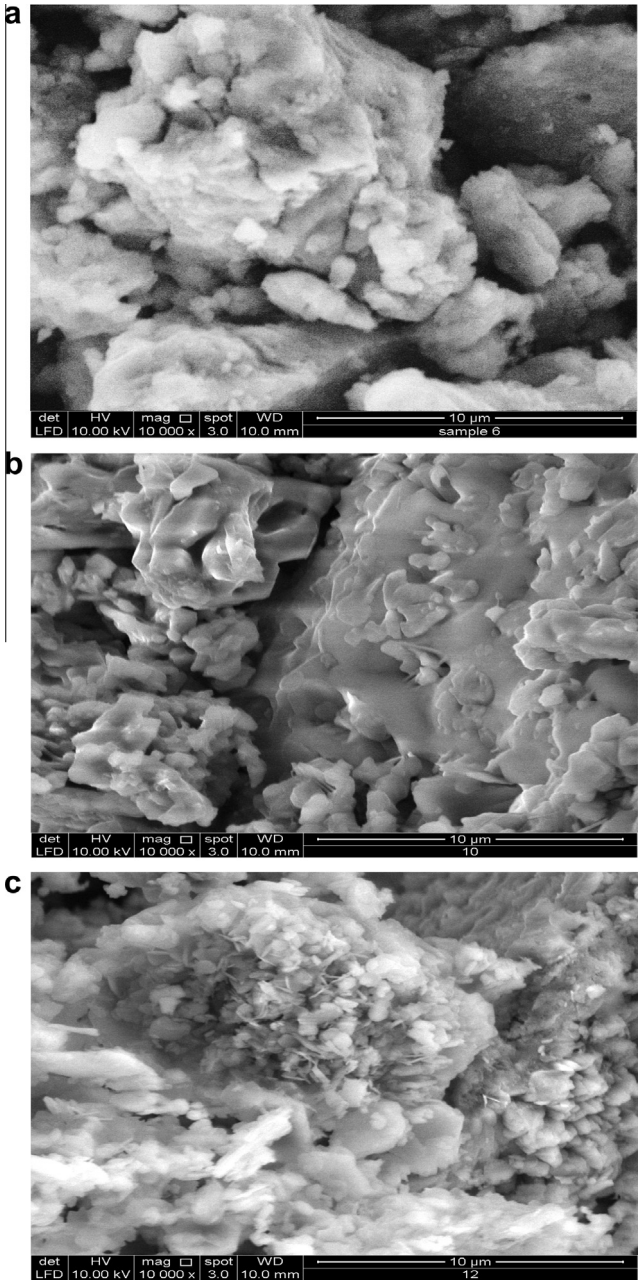

Fig. 2. (a) SEM of the HC_1 samples, (b) SEM of the HC_2 samples, and (c) SEM of the HC_4 samples.

The FTIR spectra of the HC samples, presented in Fig 3, shows the similar vibrations characteristics of the LDH structures. These include the band of H–O–H bending in water molecule at 1550–1700 cm^{-1} and the vibrations of metal-O (or metal-OH) bond at 500–750 cm^{-1}. The strong overlapping bands at 3443 in HC_1, 3662 and 3641 in HC_2 and 3475 in HC_4 were attributed to the stretching vibrations of lattice water and structural OH groups in the samples. This intense and broad absorption band regions also correspond to metal-OH stretching vibrations, in this case, Al-OH_{srt} (octahedral structural hydroxyl groups). The broadening of this band has been ascribed to hydrogen bond formation [22]. The H–O–H bending vibrations of the interlayer water molecules were shown by the peak at 1631 in HC_1 and HC_2 and 1620 in HC_4. The peak at 532 in HC_1, 528 and 788 in HC_2 and 528 and 792 in HC_4 was ascribed to bending vibration of Al-OH and stretching vibration of Al-OH respectively [22]. In addition, the

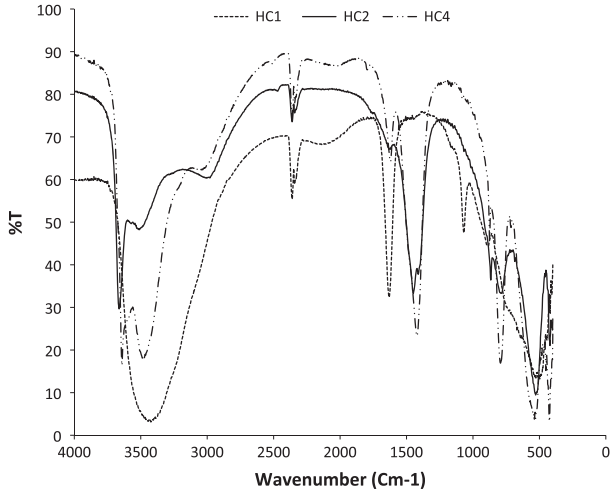

Fig. 3. FTIR spectra of the synthesized HC samples.

peak at 1448, observed in HC_2 was assigned to the anti-symmetric stretching vibration of CO_3^{2-} while the bending vibration of CO_3^{2-} was shown at 885 in HC_1, 866 in HC_2 and 873 in HC_4, The presence of CO_3^{2-} peaks was ascribed to the CO_2 captured from air during the HC preparation. No vibration peaks of chloride ions appear in the range of 400–4000 cm^{-1} due to the ionic nature of the chloride bonding with the positive charge layer.

The results of the determination of the pH_{PZC} of the HC samples (Sup. Inf. Fig. 1) shows that the pH_{PZC} of HC_1 (pH = 3.8) was lower than the pH_{PZC} values of the HC_2 and HC_4 (pH = 12.0) samples. This showed that the nature of surface charge of sample HC_1 differ, at different pH values, from that of samples HC_2 and HC_4. The pH_{PZC} values of samples HC_2 and HC_4 showed that the surface charges were predominantly positively over the pH range studied (2–12), while HC_1 surface was predominantly positive, until pH 3.8, when the surface charge changed and became predominantly negative.

3.2. Sorption studies

The concentration–time profile of the sorption of phosphate by each of the synthesized HC was assessed at different initial phosphate concentrations that ranged between 25 and 300 mg/L to establish the effects of contact time on the sorption process and to quantify the rate of phosphate uptake by the synthesized HC. This study showed that the rate of phosphate uptake from solution by the three sorbents was very fast and the percentage of residual phosphate uptake was >98% within the first 5 min of studies, for all the initial concentration studied (Sup. Inf. Figs. 2–4). The kinetic parameters for the sorption of phosphate onto the different HC samples were obtained by fitting the time–concentration profile data to the pseudo-first order and pseudo-second order kinetic models viz:

$$\log[q_e - q_t] = \log[q_e] - \left[\frac{k_1}{2.303}\right]t \quad (1)$$

$$\frac{t}{q_t} = \frac{1}{kq_e} + \frac{1}{q_e}t \quad (2)$$

The results of the kinetic analysis, presented in Table 1a revealed that, using linear coefficient value (r^2) as measure of conformance to the kinetic model, the pseudo second order gave the best description of the sorption process. The linear coefficient value was high (r^2 = 1.000) in all the cases studied. Despite the extremely high r^2 value exhibited by the different HC samples in phosphate sorption,

Table 1a
Kinetic parameters of sorption of phosphate on HC samples.

Initial conc. (mg/L)	Pseudo first order			Pseudo second order		
	q_e	k_1	r^2	q_e	k_2	r^2
HC_1						
25	1.506	0.048	0.6686	12.39	2.63	1.000
50	1.934	0.074	0.5045	24.51	4.34	1.000
100	3.355	0.052	0.7896	49.50	3.74	1.000
200	3.095	0.019	0.4735	99.01	4.81	1.000
300	11.182	0.033	0.5191	149.25	1.68	1.000
HC_2						
25	0.564	0.073	0.7776	12.52	7.68	1.000
50	0.809	0.049	0.5283	24.94	8.35	1.000
100	1.574	0.038	0.6099	50.00	7.69	1.000
200	4.175	0.069	0.5216	100.00	7.14	1.000
300	7.076	0.053	0.6242	149.25	5.58	1.000
HC_4						
25	0.794	0.090	0.7001	12.42	6.94	1.000
50	1.603	0.066	0.5424	25.00	5.71	1.000
100	2.286	0.059	0.4312	50.00	6.25	1.000
200	4.609	0.113	0.6913	100.00	5.26	1.000
300	5.026	0.056	0.5389	149.25	5.58	1.000

only the values of the equilibrium sorption capacity (q_e, mg/g), obtained from the pseudo second order plot, displayed dependency on the initial phosphate solution concentration but the pseudo second order rate of sorption (k_2) exhibited no defined trend, when the values were matched with the initial solution phosphate.

Many experimental studies have revealed that the value of k_2 strongly depends on the applied operating conditions. The k_2 constant value has been reported to be strongly dependent on the applied initial solute concentration [23]. It decreases with the increasing initial sorbate concentrations as a rule, which is a commonly known fact related to the interpretation of k_2 as a time-scaling factor (obviously, the higher is the initial sorbate concentrations value, the longer time is required to reach an equilibrium) [24–26]. Despite the widely reported dependency of k_2 values on the initial sorbate concentration, reports of systems for which k_2 is independent of initial solute concentration have also been reported [27–33]. The reported conflicting trends in the relationship between k_2 and the initial sorbate concentrations was explicated via a theoretical analysis of kinetic models of sorption by Azizian et al. [34] that for the system that obeys the pseudo-second order kinetic model, their observed rate constant is a complex function of initial concentration of solute.

Premised on the opinion of Wu et al. [35], the parameter, k_2q_e (min^{-1}) can used to define kinetic performance. This parameter was obtained by rearranging Eq. (3) to give Eq. (4) viz:

$$\frac{dq_t}{d_t} = k_2(q_e - q_t) \quad (3)$$

$$\frac{dq_{t/q_e}}{d_t} = k_2q_e\left[1 - \frac{q_t}{q_e}\right]_2 \quad (4)$$

Eq. (4) reveals that the time changes in dimensionless solid-phase concentration, $d(q_t/q_e)/d_t$, which is another form of sorption rate, is proportional to the square of the residual amount of sorbate, $1 - (q_t/q_e)$. Consequently, the proportionality constant k_2q_e can be defined as the second order rate index. Eq. (2) can be rewritten as:

$$\left(\frac{1}{q_t} - \frac{1}{q_e}\right)t = \frac{1}{k_2q_e^2} \quad (5)$$

and

$$t = \frac{\frac{q_t}{(q_e - q_t)}}{k_2q_e} \quad (6)$$

At the half-life of the sorption process (*i.e.*, $t = t_{0.5}$), we have $q_t = 0.5q_e$ and

$$t_{0.5} = \frac{1}{k_2 q_e} \tag{7}$$

The values for pseudo-second order rate index, k_2q_e (Table 1b) determined for HC-phosphate system, increased with increase in the initial phosphate solution concentration while the half-life of the sorption process reduced with increase in the initial phosphate concentrations. This showed that the half-life of the phosphate sorption onto HC was attained faster at higher initial phosphate concentrations than at lower phosphate concentrations.

An overview of the results obtained from the kinetic studies showed that the magnitude of the residual phosphate in the aqueous solution was independent of the initial phosphate concentrations. The principle of constant solubility product surmised that, if precipitation is occurring, all the residual contaminant concentration after precipitation should be in the same range, regardless of the initial concentration and interfering ions. In the light of this, the role of precipitation as a participating mechanism of removal of phosphate by the HC was studied via the determination of the saturation index (SI) values of the possible insoluble species obtainable from process.

Considering the active ionic species in solution, Ca^{2+}, Al^{3+} and PO_4^{2-}, the simplest insoluble phosphate species that can be produced from the interactions within the system were used as model insoluble phosphate salts (i.e. $Ca_3(PO_4)_2$ and $AlPO_4$ with K_{sp} values of 2.07×10^{-33} and 9.84×10^{-21}, respectively). The SI values of $Ca_3(PO_4)_2$ and $AlPO_4$ were estimated by monitoring the time–concentration profiles of the activities of the three ionic species (i.e. Ca^{2+}, Al^{3+} and PO_4^{2-}) in solution, using HC_2 as a model sorbent, in a batch process, at different initial phosphate solution concentrations of 100, 200 and 300 mg/L. Samples were withdrawn, intermittently, between 2 and 180 min and the Ca^{2+}, Al^{3+} and PO_4^{2-} activities were determined at each sampling time. The SI of each insoluble phosphate species were calculated using Eq. (8) [36] viz:

$$\mathrm{SI} = \log_{10}\left(\frac{(\text{activity of } Ca^{2+})(\text{activity of } po_4^{3-})}{\text{solubility product of } ca_3(po_4)_2}\right) \tag{8}$$

The plots of the SI value against time at the different initial solution phosphate concentrations are presented in Fig. 4a and b. The SI values for the $Ca_3(PO_4)_2$ and $AlPO_4$ were all positive and varied. The SI values of $Ca_3(PO_4)_2$ was higher (range between 34.53 and 35.54) than that of the $AlPO_4$ (ranged between 21.51 and 22.62). The SI values of the two insoluble phosphate salts increased over time and with increase in the initial solution phosphate concentrations. The increase in the SI value with increase in initial solution phosphate concentration was ascribed to the difference in the initial solution pH (The pH of the different initial phosphate concentrations of 100, 200 and 300 mg/L were 5.52, 4.98 and 4.16 respectively) exhibited by the different initial phosphate solution concentrations,

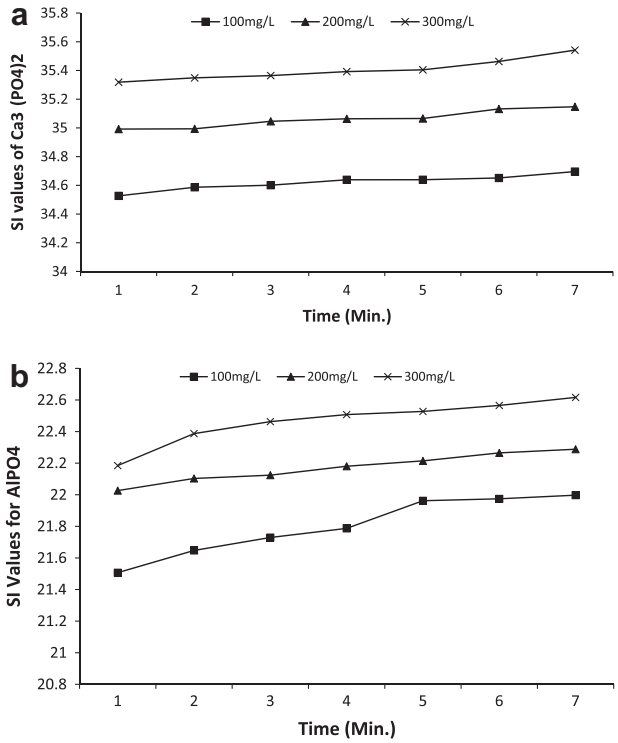

Fig. 4. (a) Plot of SI value of $Ca_3(PO_4)_2$ at different initial phosphate concentrations against time and (b) plot of the SI values of $AlPO_4$ at different initial phosphate concentration against time.

which is assumed to affect the stability of the HC samples in the aqua medium to different extent and ultimately influenced the SI values obtained from each experiment. A positive SI value has been attributed to supersaturation of the ionic species in solution which lead to precipitate formation. On the other hand, a negative SI is an indication of a dominant adsorption process [37].

Song et al. [38] proposed that SI value is a good indicator to show the deviation of a salt from its equilibrium state, i.e. the thermodynamic driving force for precipitation to occur. But considering the kinetics, supersaturation does not certainly mean the quick occurrence of a spontaneous precipitation. Between the undersaturated zone and spontaneous precipitation zone there is still a metastable zone, where the solution is already supersaturated but no precipitation occurs over a relatively long period [39]. The boundary between metastable zone and spontaneous precipitation zone can be called the critical supersaturation [40]. The thermodynamic driving force to a chemical reaction is the Gibbs free energy ΔG (kJ/mol), and it is the criterion to judge whether a reaction is spontaneous, in equilibrium, or impossible, corresponding to $\Delta G < 0$, =0, or >0, respectively. The Gibbs free energy of a precipitation reaction is given by [38]:

Table 1b
Determination of the sorption performance of HC for Phosphate sorption using pseudo second order model.

Pseudo 2nd order parameters	25 mg/L	50 mg/L	100 mg/L	200 mg/L	300 mg/L
HC_1					
k_2q_e	32.586	106.373	185.130	476.238	250.74
$t_{0.5}$	0.031	0.009	0.005	0.002	0.004
HC_2					
k_2q_e	96.154	208.249	384.500	714.000	832.815
$t_{0.5}$	0.010	0.005	0.003	0.001	0.001
HC_4					
k_2q_e	86.195	142.750	312.500	526.000	832.815
$t_{0.5}$	0.012	0.007	0.003	0.002	0.001

$$\Delta G = -\frac{RT}{n}\ln\frac{IAP}{K_{sp}} \quad (9)$$

where R is the ideal gas constant, T is the absolute temperature, IAP and K_{sp} are, respectively, the free ionic activities product and the thermodynamic solubility product of the precipitate phase and, n, is the number of ions in the precipitated compound.

In order to judge supersaturation, which is a measure of the deviation of a dissolved salt from its equilibrium value, the SI of a solution with respect to a precipitate phase is defined.

$$SI = \log\frac{IAP}{K_{sp}} \quad (10)$$

Therefore

$$\Delta G = -\frac{2.303RT}{n}SI \quad (11)$$

when SI = 0, hence $\Delta G = 0$, the solution is in equilibrium; when SI < 0, $\Delta G > 0$, the solution is undersaturated and precipitation is impossible; when SI > 0, $\Delta G < 0$, the solution is supersaturated and precipitation is spontaneous.

The results of the thermodynamic analysis of precipitation reaction in the removal of phosphate by HC showed that the value of $\Delta G < 0$ and ranged between −110071.31 and −113307.00 for $Ca_3(PO_4)_2$ and −68563.36 and −72100.40 for $AlPO_4$ formations, over the entire period of the sorption process, which is an indication that the precipitation of phosphate inform of the insoluble Ca^{2+} and Al^{3+} salt were feasible and also a paramount contributory mechanism of phosphate removal in the batch process. The occurrence of both adsorption and precipitation as a mechanism of aqua phosphate removal has been postulated by different researchers in the use of calcium rich material as sorbent [41–45].

The influence of the ratio of the constituents of the HC samples on equilibrium isotherm parameters were appraised via equilibrium isotherm analysis of the sorption process. The data obtained from the equilibrium isotherm studies were fitted to the two conventionally used equilibrium isotherm equations, represented by the following linear equations, viz:

$$\text{Langmuir}: \frac{c_e}{q_e} = \frac{1}{q_m}c_e + \frac{1}{k_a q_m} \quad (12)$$

$$\text{Freundlich}: \log q_e = \log k_f + \frac{1}{n}\log c_e \quad (13)$$

The values of the Langmuir monolayer sorption capacities, q_m (mg/g), obtained (Table 2) for the synthesized sorbent were in the same range (208.33–212.76 mg/g) but HC_2 had the highest (212.76 mg/L). Both equilibrium sorption isotherm equations had relatively high linear correlation coefficient values (r^2) but that of the Langmuir isotherm equation was higher in the three samples.

3.3. Effect of initial solution pH

The effects of initial solution pH on the removal of phosphate from aqua system was studied using HC_2 at fixed solution phosphate concentration of 200 mg/L but different initial solution pH that ranged between 7 and 10. This pH ranged was chosen to prevent the dissolution of the constituents of the HC which are known not to be stable at acidic pH. The results obtained (Fig. 5) showed a slight increase in the magnitude of phosphate removed with increase in solution pH. The equilibrium solution pH (pH_f), determined at the end of the sorption process (Fig. 5) in each case, was higher than the initial solution pH, within the pH range studied. The results of the PZC of the different HC samples showed that the predominant surface charge on samples HC_2 and HC_4 were positive charges, within the pH range studied, while the surface charge on HC_4 was negative until pH 3.8 when the predominance of positive charges took place. Considering the similarities displayed in the magnitude of phosphate removed from solution by the three HC samples, it is very glaring that ionic interaction could not have been the mechanism of phosphate removal from solution, even if adsorption played a key role in the phosphate removal by the HC samples.

Table 2
Equilibrium isotherm parameters for the removal of phosphate by HC.

Samples	Langmuir			Freundlich		
	q_m	kL	r^2	$1/n$	k_f	r^2
HC_1	208.33	1.412	0.9946	0.6835	119.99	0.9682
HC_2	212.76	0.560	0.9957	0.6885	64.98	0.9809
HC_4	208.33	1.231	0.9837	0.6949	110.01	0.9579

3.4. Effects of organic load

The effects of the presence of organics, which is a normal occurrence in wastewater, were simulated via the addition of humic acid (HA) of varying concentrations to a fixed concentration (200 mg/L) of phosphate solution, using the HC_2 sample as sorbent. The effects of the presence of different concentrations of HA on the removal of phosphate are presented in Fig. 6. The amounts (mg/L) of residual phosphate in the treated water were in the same range (2.98–3.02), despite the variation in the organic load (HA dosage range: 5–80 mg/L) of the phosphate contaminated water.

The simultaneous removal of the organic constituents by the HC was also studied via the determination of the residual HA concentration after the sorption process. After the quantification of the

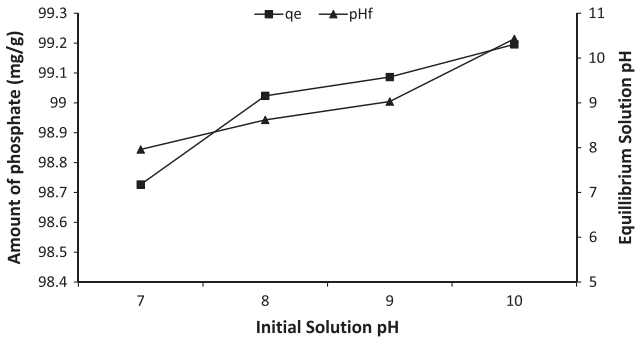

Fig. 5. Effects of initial solution pH on the removal of phosphate from aqua system using HC_2.

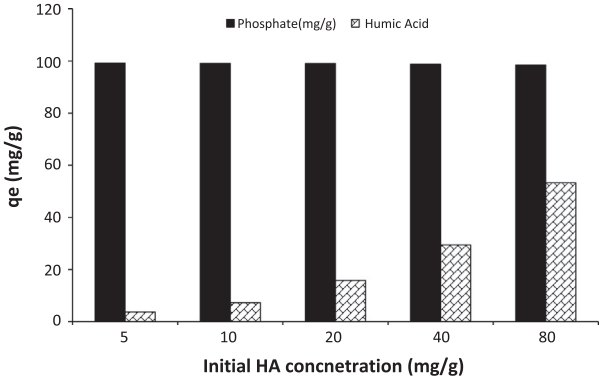

Fig. 6. Effects of organic load on the removal of phosphate from aqua system and simultaneous removal of humic acid.

residual phosphate in the supernatant, another portion of the supernatant was filtrated through a 0.45 μm filtration membrane to measure the UV_{254} absorbance at a 254 nm wavelength with a UV–VIS spectrophotometer. The estimation of UV_{254} absorbance in the treated water was used to evaluate the simultaneous organic matter removal efficiency of the sorption process (Fig. 6). The relationship between UV_{254} absorbance and HA concentration was determined and found to be linear as shown (results not shown for concision), thereby constituting a basis of conversion of UV_{254} absorbance data to an equivalent HA concentration. The amount of HA removed increased from 3.72 mg/g to 53.31 mg/g as the initial concentration of the HA increased from 5 mg/L to 80 mg/L at fixed phosphate concentration (200 mg/L). This showed that organic load is simultaneously abstracted with the phosphate molecules from the aqua system by the HC.

Humic acid (HA) is one of the major components of humic substances which contain both hydrophilic and hydrophobic molecules as well as many functional groups such as carboxyl, phenolic and hydroxyl groups connected to a skeleton of aliphatic or aromatic units. Anirudhan et al. [46] opined that the carboxylic and phenolic group on the HA are deprotonated in weakly acidic to basic media thereby conferring negative charge on the HA molecule. If ionic interaction between the HC surface and the phosphate molecules was the mechanism of interaction, the HA molecules is expected to be repelled from the HC surface, taken into cognizance the very high pH_{PZC} value of the HC_2 sample, and competition between the HA molecules and the phosphate molecules (which are both negatively charged) for oppositely charged site (positively charged sites) on the HC and this would have manifested in substantial reduction in the amount of phosphate removed by the HC, with increase in the HA concentration. In the present study, considerable amount of the HA was removed simultaneously with the phosphate molecules, which lend credence to the non-participatory role of ionic interaction in phosphate removal by the HC samples. It is assumed that if precipitation was the controlling mechanism, the removal of the HA must have occurred via sweep coagulation during the formation of the insoluble phosphate salts of calcium and aluminum.

3.5. Effect of ionic strength

In the present study, phosphate contaminated waters of fixed concentration (200 mg/L) were prepared in solutions of NaCl of different concentrations, equivalent to the solution of following ionic strengths: 0.02; 0.04; 0.09; 0.17 and 0.43. The amount of phosphate removed marginally reduced with increase in the phosphate solution ionic strength (Sup. Info. Fig. 5). Analogous results have been reported by Bowden et al. [47], Chouyyok et al. [48], and Yin et al. [49] who performed phosphorus sorption studies using slag, Fe-rich material, and calcium rich sepiolite respectively, as sorbents. Chitrakar et al. [50] ascribed the nominal influence of salinity on the phosphate uptake of δ-MnO_2 in seawater to the presence of two kinds of adsorptive sites on the sorbent: non-specific sites with weak interaction and specific ones that strongly interact with phosphate ions. The non-specific sites may be sensitive to the coexisting anions, and therefore the adsorbed phosphate may be easily exchangeable with either Cl^- or SO_4^{2-} in the solution phase, even at low salinity. On the other hand, the phosphate ions adsorbed on the strong specific sites may be rarely exchangeable even in a solution with a large excess amount of coexisting ions.

Albeit, the influence of ionic strength was nominal in the phosphate uptake in the present study, but the presence of two adsorptive sites may not be enough reason for the observed influence if the evidences from the other studies undertaking in the present research are considered and the principle of constant solubility product is also taken into perception.

3.6. Fractionation of the P-saturated absorbent

Studies have shown that excellent and efficient phosphorus absorbents are characterized by their high aluminum, iron or calcium contents. This has made substrates with high contents of these elements to be phosphorus-removing absorbents. The sorbent used in the present studies HC, is made up of two elements that have strong affinity for phosphorus. The phosphorus fractionation protocol was employed to elucidate the role of each constituent of the sorbent in the phosphorus abstraction from aqueous solution to provide insight into the possible mechanisms of phosphate removal from the aqua system.

The different forms of bound phosphorus determined in the spent HC_2 include Ca_2-P, Ca_8-P, Ca_{10}-P and Al-P. The order of distribution of each fraction of P, relative to the total phosphorus (T-P) in the phosphate laden HC, is as follows: Ca_2-P (44.64%) > Ca_{10}-P (40.23%) > Ca_8-P (14.64%) > Al-P (0.49%). Yin et al. [49] ascribed the relatively high percentage of Ca bound phosphorus to the role of precipitation as the mechanism of phosphate removal in a system. Reports on the distribution and forms of phosphorus association in used constructed wetland substrate [51,52] have also shown that large amount of P sorbed onto the surface of blast furnace slag is predominantly associated with light elements, such as calcium, aluminum, magnesium and silicon, with calcium hydroxide found to absorb the largest amount of P. In the present study, the sorbent HC comprises of Ca^{2+} and Al^{3+} but the phosphorus was mainly distributed in the calcium phase which is a further confirmation of the role of precipitation in the phosphate abstraction.

3.7. Characterization of phosphate laden HC

The characterization of the phosphate laden sorbent was performed to elucidate the nature of interaction and changes that took place in the adsorbent with the uptake of phosphate from the aqua system. An appraisal of the FTIR spectra of both the virgin HC_2 and phosphate laden HC_2 (PHC_2) (Sup. Inf. Fig. 6) revealed the appearance of new peaks and alteration in the previous peaks shown by the virgin HC. The sharp intense peak at 3662 and the shoulder at 3518, attributed to the OH stretching vibration and the Al-OH vibration was replaced with a sharp intense broad band of three different peaks at 3620, 3527 and 3471. In the HC sample, the peaks at 788, due to the stretching vibration of Al-OH got shifted to 796 and the peak at 528, attributed to the bending vibration of Al-OH disappeared and got replaced with phosphate peaks. The presence of phosphate phase was confirmed by the appearance of phosphate peaks (cm^{-1}) at 520, 557, 966.37 and 1028. The presence of bands between 1200 and 900 has been ascribed to the presence of interfacial phosphate [53]. The HC sample, after phosphate adsorption, showed a characteristic band around 1028, which is an indication of the presence of deprotonated phosphate (free PO_3^{4-}) in the interlayer or surface [54].

The XRD of the HC_2, when compared with that of the PHC_2 (Fig. 7), showed significant reduction in the crystallinity and total disappearance of some of the HC peaks after phosphate uptake. This significant reduction was ascribed to the formation of amorphous phosphate salts of Ca and Al on the surface of the HC. The size of the particles of the PHC_2 was also determined, using the Scherrer equation, and the average grain size was 97 nm, which was lower than that of the HC_2 (116 nm).

The results of the SEM (Fig. 8a) analysis showed a complete transformation of the surface architecture which suggests the formation of a new compound on the surface of the HC during phosphate uptake. The results of the EDAX (Fig. 8b) showed the appearance of phosphorus peaks amongst the element detected in HC. An important feature of the EDAX results is the significant

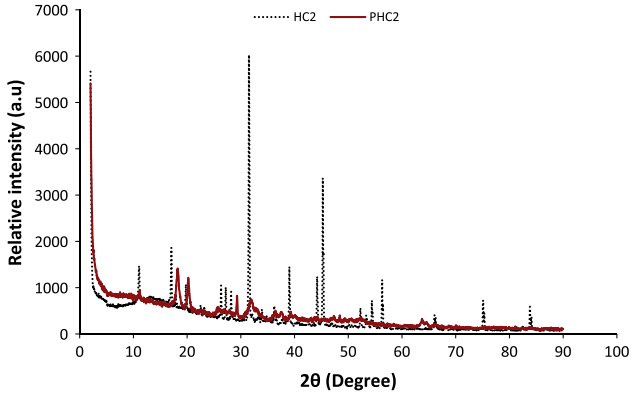

Fig. 7. XRD of HC_2 and PHC_2 samples.

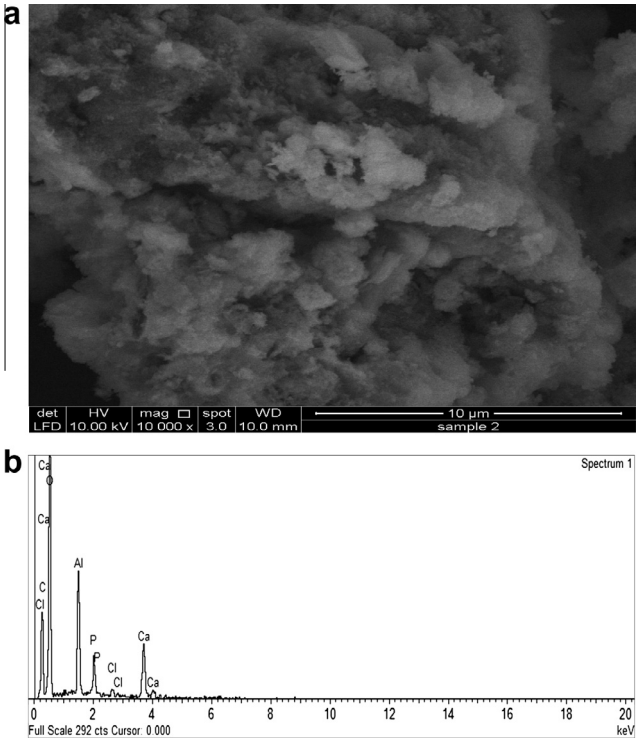

Fig. 8. (a) SEM analysis of the PHC_2 samples and (b) EDAX analysis of the PHC_2 samples.

reduction in the intensity of the chlorine peak of the PHC_2 when compared with that of the HC_2 which is an indication of ion exchange between chlorine and phosphate in the aqua system.

Layered double hydroxides or hydrotalcite-like material possess intrinsic anion uptake capacity because of the presence of facile exchangeable interlayer anions (in this case Chloride) and large external surface which has made them to be material of choice in oxyanion attenuation in aqua system. The results of the fitting of the time–concentration profile data into pseudo second order model revealed an extremely high correlation coefficient value ($r^2 = 1.000$) which is an indication of the role of chemisorption mechanism of sorption in phosphate removal by the HC samples but the non-dependency of one of the pseudo second order parameters cast doubt on the overall applicability of this kinetic model to the sorption process. Consequent upon the inherent anion uptake ability of the HC, the partial applicability of the pseudo second order kinetic model and the results from the EDAX, it could be assumed that anion exchange is also a player in phosphate removal by the HC.

The role of precipitation in phosphate removal by the HC has been confirmed from the results from the different studies undertaken herein. Consequently, it could be concluded that the removal of phosphate by the HC could not have occurred via a single mechanism but a combination of adsorption (specifically anion exchange) and precipitation.

4. Conclusion

- The shell of Gastropod could be used as a precursor for the synthesis of Nano-sized hydrocalumite.
- The removal of phosphate by the synthesized hydrocalumite sample occurred fast and was independent of initial phosphate solution concentrations.
- The pseudo second order rate constant (k_2) derived from the sorption process was independent of the initial phosphate solution concentrations.
- Process variables optimization (pH, ionic strength and organic load) had nominal influence on the magnitude of phosphate removal.
- The formation of supersaturated phosphate salt of calcium and aluminum was confirmed by the positive saturation index value and precipitate formation was confirmed by the thermodynamic parameter.
- 99% of the phosphate abstracted by the synthesized hydrocalumite was distributed in the calcium phase.

Acknowledgement

The authors wish to express gratitude to the International Foundation for Science (IFS), Sweden, for the renewal Grant (W/4212-2) awarded to Nurudeen Abiola OLADOJA to undertake this research.

Appendix A. Supplementary material

Supplementary material associated with this article can be found, in the online version, at http://dx.doi.org/10.1016/j.seppur.2014.01.018.

References

[1] S.P. Gao, T.H. Lu, S.P. Li, H. Zhong, The mechanism on the pH value influencing the property of glutamic acid/layered double hydroxide compounds, Colloids Surf., A 351 (2009) 26–29.
[2] P.C. Pavan, E.L. Crepaldi, J.B. Valim, J. Colloid Interface Sci. 229 (2000) 346.
[3] I. Baur, C.A. Johnson, The solubility of selenate-Aft ($3CaO{\cdot}Al_2O_3{\cdot}3CaSeO_4{\cdot}37.5H_2O$) and selenate–AFm ($3CaO{\cdot}Al_2O_3{\cdot}CaSeO_4{\cdot}xH_2O$), Cem. Concr. Res. 33 (2003) 1741–1748.
[4] I. Baur, C.A. Johnson, Sorption of selenite and selenate to cement minerals, Environ. Sci. Technol. 37 (2003) 3442–3447.
[5] I. Bonhoure, I. Baur, Uptake of Se (IV/VI) oxyanions by hardened cement paste and cement minerals: an X-ray absorption spectroscopy study, Cem. Concr. Res. 36 (2006) 91–98.
[6] M. Chrysochoou, D. Dermatas, Evaluation of ettringite and hydrocalumite formation for heavy metal immobilization: literature review and experimental study, J. Hazard. Mater. 136 (2006) 20–33.
[7] E.A. Johnson, M.J. Rudin, S.M. Steinberg, W.H. Johnson, The sorption of selenite on various formulations, Waste Manage. 20 (2000) 509–516.
[8] D. Peak, D.L. Sparks, Mechanisms of selenate adsorption on iron oxide and hydroxide, Environ. Sci. Technol. 36 (2002) 1460–1466.
[9] R.P.J.J. Rietra, T. Hiemstra, W.H. Riemsdijk, Comparison of selenate and sulfate adsorption on goethite, J. Colloid Interface Sci. 240 (2001) 384–390.
[10] M. Zhang, E.J. Reardon, Removal of B, Cr, Mo, and Se from wastewater by Incorporation into hydrocalumite and ettringite, Environ. Sci. Technol. 37 (2003) 2947–2952.
[11] Y. Wu, Y. Chi, H. Bai, G. Qian, Y. Cao, J. Zhou, Y. Xu, Q. Liu, Z.P. Xu, S. Qiao, Effective removal of selenate from aqueous solutions by the Friedel phase, J. Hazard. Mater. 176 (2010) 193–198.

[12] N.A. Oladoja, Y.D. Aliu, Snail shell as coagulant aid in the alum precipitation of malachite green from aqua system, J. Hazard. Mater. 164 (2009) 1494–1502.
[13] N.A. Oladoja, Y.D. Aliu, A.E. Ofomaja, Evaluation of Snail shell as coagulant aid in the alum precipitation of aniline blue from aqua system, Environ. Technol. 32 (6) (2011) 639–652.
[14] N.A. Oladoja, I.A. Ololade, A.O. Adesina, R.O.A. Adelagun, Y.M. Sani, Appraisal of gastropod shell as calcium ion source for phosphate removal and recovery in calcium phosphate minerals crystallization procedure, Chem. Eng. Res. Des. 91 (5) (2013) 810–818.
[15] N.A. Oladoja, A.L. Ahmad, Gastropod shell as a precursor for the synthesis of binary alkali-earth and transition metal oxide for Cr(VI) abstraction from aqua system, Sep. Purif. Technol. 116 (2013) 230–239.
[16] N.A. Oladoja, I.O. Raji, S.E. Olaseni, T.D. Onimisi, In situ hybridization of waste dyes into growing particles of calcium derivatives synthesized from a Gastropod shell (*Achatina achatina*), Chem. Eng. J. 171 (2011) 941–950.
[17] S.K. Milonjic, A.L.J. Ruvarac, M.V. Susić, The heat of immersion of natural magnetite in aqueous solutions, Thermochim. Acta 11 (3) (1975) 261.
[18] N.A. Oladoja, C.O. Aboluwoye, A.O. Akinkugbe, Evaluation of loofah as a sorbent in the decolorization of basic dye contaminated aqueous system, Ind. Eng. Chem. Res. 48 (2009) 2786–2794.
[19] S.C. Chang, M.L. Jackson, Fractionation of soil phosphorus, Soil Sci. 84 (1957) 133–144.
[20] Y.C. Gu, B.F. Jiang, A method for fractionation of inorganic phosphorus of calcareous soils, Soils 22 (1990) 101–102 (in Chinese).
[21] J. Zhou, Y. Cheng, J. Yu, G. Liu, Hierarchically porous calcined lithium/aluminum layered double hydroxides: facile synthesis and enhanced adsorption towards fluoride in water, J. Mater. Chem. 21 (2011) 19353–19361.
[22] U.A. Birnin-Yauri, F.P. Glasser, Friedel's salt $Ca_2Al(OH)_6(Cl, OH)\cdot 2H_2O$: its solid solution and their role in chloride binding, Cem. Concr. Res. 28 (1998) 1713–1723.
[23] W. Plazinski, W. Rudzinski, A. Plazinska, Theoretical models of sorption kinetics including a surface reaction mechanism: a review, Adv. Colloid Interface Sci. 152 (2009) 2–13.
[24] J. Febrianto, A.N. Kosasih, J. Sunarso, Y.H. Ju, N. Indraswati, S. Ismadji, J. Hazard. Mater. 162 (2009) 616.
[25] S.R. Popuri, Y. Vijaya, V.M. Boddu, K. Abburi, Biores. Technol. 100 (2009) 194.
[26] M.A. Al-Ghouti, M.A.M. Khraisheh, M.N.M. Ahmad, S. Allen, J. Hazard. Mater. 165 (2009) 589.
[27] R. Aravindhan, N.N. Fathima, J.R. Rao, B.U. Nair, Colloids Surf., A 299 (2007) 232.
[28] D. Kavitha, C. Namasivayam, Biores. Technol. 98 (2007) 14.
[29] M. Alkan, O. Demirbas, M. Dogan, Microporous Mesoporous Mater. 101 (2007) 388.
[30] Y. Vijaya, S.R. Popuri, V.M. Boddu, A. Krishnaiah, Carbohyd. Polym. 72 (2008) 261.
[31] J. Yu, M. Tong, X. Sun, B. Li, J. Hazard. Mater. 143 (2007) 277.
[32] P.X. Sheng, K.H. Wee, Y.P. Ting, J.P. Chen, Chem. Eng. J. 136 (2008) 156.
[33] N. Ertugay, Y.K. Bayhan, J. Hazard. Mater. 154 (2008) 432.
[34] S. Azizian, Kinetic models of sorption: a theoretical analysis, J. Colloid Interface Sci. 276 (2004) 47–52.
[35] F.C. Wu, R.L. Tseng, R.S. Juang, Initial behavior of intraparticle diffusion model used in the description of adsorption kinetics, Chem. Eng. J. 153 (2009) 1–8.
[36] S.K. Nath, R.K. Dutta, Acid-enhanced limestone defluoridation in column reactor using oxalic acid, Process Saf. Environ. Prot. 90 (2012) 65–75.
[37] B.D. Turner, P.J. Binning, S.L.S. Stipp, Fluoride removal by calcite: evidence for fluoride precipitation and surface adsorption, Environ. Sci. Technol. 39 (2005) 9561–9568.
[38] Y. Song, H.H. Hahn, E. Hoffmann, Effects of solution conditions on the precipitation of phosphate for recovery a thermodynamic evaluation, Chemosphere 48 (2002) 1029–1034.
[39] W. Stumm, J.J. Morgan, Aquatic Chemistry, third ed., John Wiley & Sons, Inc., New York, 1996, p. 356.
[40] I. Joko, Phosphorus removal from wastewater by the crystallization method, Water Sci. Technol. 17 (1984) 121–132.
[41] W.L. Lindsay, Phosphate Chemical Equilibria in Soils, John Wiley & Sons, Inc., 1979, pp. 162–209.
[42] C.J. Richardson, Mechanisms controlling P retention capacity in fresh water wetlands, Science 228 (1985) 1424.
[43] S.P. Faulkner, B.C. Richardson, Physical and chemical characteristic of freshwater wetlands, in: D.A. Hammer (Ed.), Constructed Wetlands for Wastewater Treatment: Municipal, Industrial and Agricultural, Lewis Publishers, Chelsea, 1989, pp. 41–72.
[44] E. Oguz, Removal of phosphate from aqueous solution with blast furnace slag, J. Hazard. Mater. B114 (2004) 131–137.
[45] J. Zhou, Z.P. Xu, S. Qiao, Q. Liu, Y. Xu, G. Qian, Enhanced removal of triphosphate by MgCaFe–Cl–LDH: synergism of precipitation with intercalation and surface uptake, J. Hazard. Mater. 189 (2011) 586–594.
[46] T.S. Anirudhan, P.S. Suchithra, S. Rijith, Amine-modified polyacrylamide bentonite composite for the adsorption of humic acid in aqueous solutions, Colloids Surf., A 326 (2008) 147–156.
[47] L.I. Bowden, A.P. Jarvis, P.L. Younger, K.L. Johnson, Phosphorus removal from waste waters using basic oxygen steel slag, Environ. Sci. Technol. 43 (2009) 2476–2481.
[48] W. Chouyyok, R.J. Wiacek, K. Pattamakomsan, T. Sangvanich, R.M. Grudzien, G.E. Fryxell, Phosphate removal by anion binding on functionalized nanoporous sorbents, Environ. Sci. Technol. 44 (2010) 3073–3078.
[49] H. Yin, Y. Yun, Y. Zhang, C. Fan, Phosphate removal from wastewaters by a naturally occurring, calcium-rich sepiolite, J. Hazard. Mater. 198 (2011) 362–369.
[50] R. Chitrakar, S. Tezuka, A. Sonoda, K. Sakane, K. Ooi, T. Hirotsu, Selective adsorption of phosphate from seawater and wastewater by amorphous zirconium hydroxide, J. Colloid Interface Sci. 297 (2006) 426–433.
[51] K. Sakadevan, H.J. Bavor, Phosphate adsorption characteristics of soils, slags and zeolite to be used as substrates in constructed wetland systems, Water Res. 32 (2) (1998) 391–399.
[52] L. Johansson, Blast furnace slag as phosphorus sorbents—column studies, Sci. Total Environ. 229 (1) (1999) 89–97.
[53] M.I. Tejedor-Tejedor, M.A. Anderson, Langmuir 6 (1990) 602.
[54] J.T. Kloprogge, R.L. Frost, in: V. Rives (Ed.), Layered Double Hydroxides: Present and Future, Nova Science, New York, 2001, p. 153.